

## **FREQUENCY-DOMAIN SYNTHESIS OF THE FATIGUE LOAD SPECTRUM FOR THE NPS 100-KW WIND TURBINE\***

by

Herbert J. Sutherland  
Sandia National Laboratories  
Albuquerque, New Mexico 87185

and

Richard M. Osgood  
National Renewable Energy Laboratory  
Golden, CO 80401

### **ABSTRACT \***

The LIFE2 code is a fatigue/fracture mechanics code that is specialized to the analysis of wind turbine components. Two frequency-domain stress spectra techniques contained in this code are used to analyze the measured frequency loads spectra from the Northern Power Systems 100-kW turbine. Results of the two techniques are compared to cycle counts obtained directly from time series data. These results provide the wind turbine designer with two techniques for determining the cycle-counts from frequency data and illustrate the accuracy that the designer can expect from various cycle-counting techniques.

### **INTRODUCTION**

The LIFE2 code is a fatigue/fracture mechanics code that is specialized to the analysis of wind turbine components.<sup>1</sup> This code permits the analysis of both time series<sup>2</sup> and frequency domain data.<sup>3</sup> In the case of the former, a "rainflow counting" algorithm is used to convert time series data into a cycle count matrix suitable for fatigue analysis. For the latter, a Fast Fourier Transform (FFT) is used to synthesize time series data that are suitable for cycle counting using a rainflow counter.

In 1988, Northern Power Systems (NPS) erected several 100-kW turbines in Altamont Pass, California, see Figure 1. Under the auspices of the NREL (formerly SERI) Cooperative Research Program, an extensive data set was obtained for this turbine.<sup>4</sup> These data permit a detailed analysis of the frequency-

---

\* This work is supported by the U.S. Department of Energy under contract DE-AC04-76DP00789 and contract DE-FC02-86CH10311.

domain stress spectra for the turbine. And, they permit a direct comparison of the cycle count matrices from frequency domain data to cycle count matrices from time series data. This paper uses the LIFE2 code to compare two techniques to obtain cycle count matrices from frequency domain data. The first technique uses the entire frequency-domain stress spectra, an FFT and a rainflow counter. The second technique uses time series data for the deterministic (azimuth average) stresses and frequency spectra data for the non-deterministic ("random") stresses. Results of the two techniques are compared with the cycle count matrices obtained directly from time series data.

These results provide the wind turbine designer with two techniques for determining cycle counts from frequency data, and they illustrate the accuracy that the designer can expect from the various cycle-counting techniques. Moreover, these results illustrate the importance of obtaining relatively long time series data for the determination of the high-stress tail of the cycle count distribution.

## TYPICAL DATA

The data set collected by the NREL Cooperative Research Program on the NPS 100-kW turbines in Altamont Pass, California, has been described in Reference 4. The NPS horizontal axis wind turbine (HAWT) is a two-bladed, upwind, teetering hub design utilizing full-span hydraulic passive pitch control. The fiberglass rotor blades, including the elastomeric teetering hub, span 17.8 meters (rotor diameter).

The rotor's low speed shaft turns a two-stage, two-speed gearbox. The high speed shaft of the gearbox is connected to one of two fully enclosed induction generators. The present paper discusses data collected during operation of the turbine's 100-kW generator. This generator is rated at full power when rotating at 71.8 rpm in a 14 m/s wind.

Several turbine configurations were used during the collection of the NREL data set. Here, we have selected a data set for the turbine in a "locked yaw" (stiff spring) and "free teeter" with damping and stiffness. For this configuration, a 1.14-hour data segment was extracted from the main data set. During this period, the turbine was operated continuously at approximately 71.6 rpm. The average wind speed for this data set was 11.00 m/s with a turbulence factor (RMS) of 3.62 m/s. The first 400 seconds of the wind speed data are shown in Figure 2.

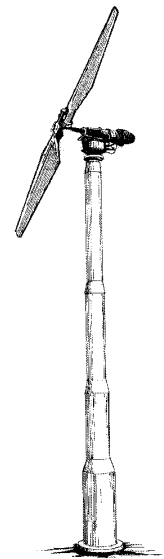


**Figure 1. The Northern Power Systems 100 k-W Turbine.**

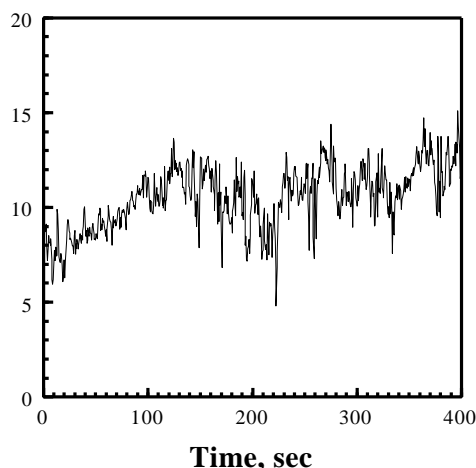


**Figure 2. The First 400 Seconds of the Wind Speed Record.**

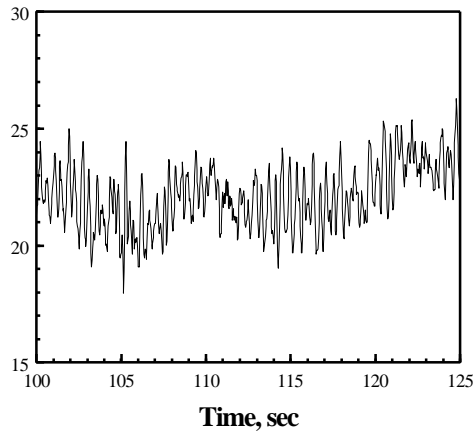


**Figure 3. Typical Root Flap Bending Moment Stress Histogram.**

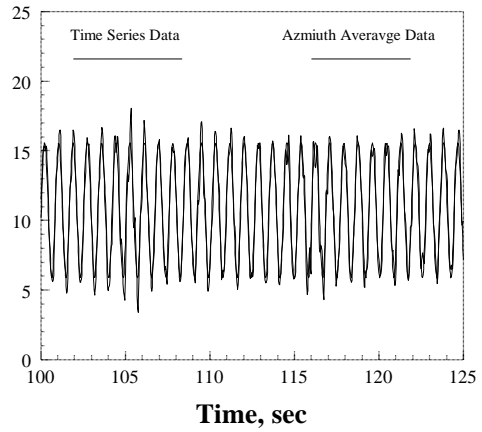


**Figure 4. Typical Root Edgewise Bending Moment Stress Histogram. The solid and dashed lines overlay one another almost everywhere.**

Data from two strain gauge channels are discussed here. The channels employ full-bridge bending configurations located on the fiberglass blades' hollow circular root shank. The first channel measures the root flap bending moment; i.e., the blades' out-of-plane bending moment. The second channel measures the root edgewise bending moment; i.e., the blades' in-plane bending moment. These two channels were reduced using the NREL data reduction package<sup>5</sup> to the stress level at the outer fibers of the blade's root. Typical stress histograms (time series data) from the selected data set are shown in Figures 3 and 4.

**RAINFLOW ANALYSIS**

Data from the two channels analyzed here were rainflow counted using the algorithm in the LIFE2 code.<sup>2</sup> Results of the analyses are shown in three-dimensional (3D) plots in Figures 5 and 6 for the root flapwise and root edgewise bending stresses, respectively. In these and subsequent cycle count plots, the number

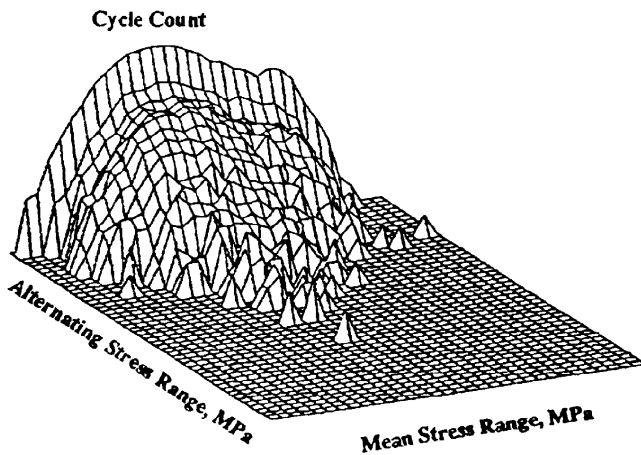


**Figure 5. Semi-Log Plots of the Cycle Counts for the Root Flap Bending Stress.**

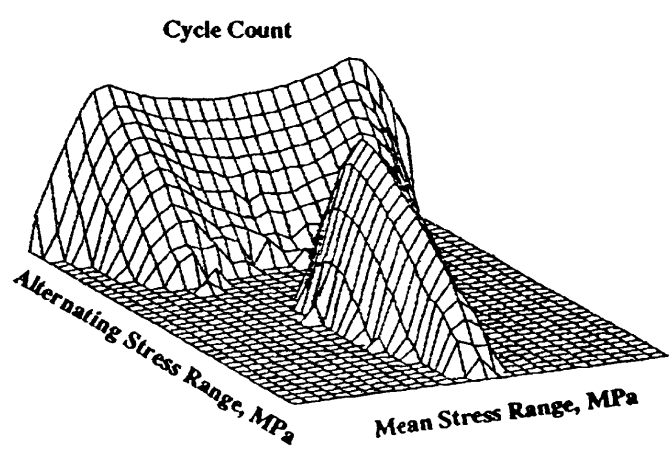


**Figure 6. Semi-Log Plots of the Cycle Counts for the Root Edgewise Bending Stress.**

of cycle counts has been normalized to 100 seconds. This normalization permits the direct comparisons of cycle counts for time series of different lengths.

As shown in these figures, the cycle count matrices have a significantly different structure. The difference in the shape of these two distributions is a direct result of the strong deterministic signal (azimuth average signal) contained in the edgewise bending data. This deterministic component is a direct result of the action of gravity on the blades. This component is shown in Figure 4 as a dashed line. These cycle counts are similar to those obtained by Thresher, Hock and Osgood.<sup>6</sup>

## SPECTRAL ANALYSIS

### Root Flap Bending Stress

A frequency-domain amplitude spectrum for the root flap bending stress is shown in Figure 7. This spectrum was obtained by applying a forward FFT<sup>3</sup> to the time series data. The entire 1.14 hours of time series data were divided into 71 segments, each 56.9-seconds long, with a sample rate of 36 samples per second; i.e., 0.028 seconds between data scans. The Nyquist Frequency for these calculations is 18 Hz, and the frequency interval is 0.018 Hz. An average spectrum was obtained using an ensemble average at each frequency in the spectrum up to 10 Hz. Above 10 Hz, the spectrum is set equal to zero (the time series data was filtered with a low-pass 10 Hz filter).<sup>4</sup>

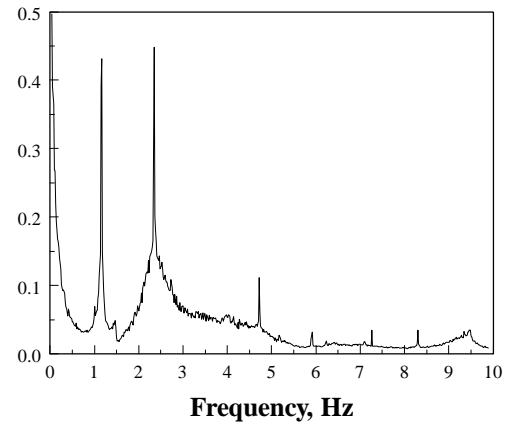


**Figure 7. Amplitude Spectrum for the Root Flap Bending Stress.**

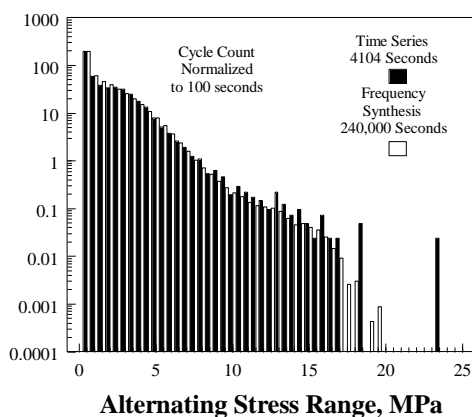


**Figure 8. Alternating Stress Cycle Count Distribution for Measured Data and Synthesized Time Series Data from Average Spectra, Root Flap Bending Stress.**

As shown in Figure 7, there are several peaks in the spectrum. The "one-per-rev" (1P) and the "two-per-rev" (2P) peaks are located near 1.2 and 2.4 Hz, respectively.

As noted in Sutherland<sup>3</sup>, the spectra may be analyzed by the LIFE2 code with or without associated phase angles and variations in the spectral amplitude. For the analysis presented in this section, the phase angles for the two peaks at approximately 1.2 and 2.4 Hz were retained.

The results for approximately 4000 sets of synthesized time series data are summarized in Figure 8. Each synthesized time series was 56.9 seconds in length. Thus, the total time synthesized for this figure is approximately of 240,000 seconds (66 hours). In this and subsequent figures, the cycle counts are plotted as a function of the alternating

stress range. Namely, the alternating-stress cycle counts have been summed over all mean stresses.

As illustrated in this figure, the synthesized data fit the body of the cycle count distribution very well. However, the high-stress tail of the distribution is not fit very well. As discussed by Sutherland<sup>3</sup> and Malcolm,<sup>7</sup> the population of cycle counts in the high-stress tail of the cycle count distribution is very important in the determination of the service lifetime of a turbine component. And, the frequency-domain technique should be able to duplicate the time series data if the spectrum contains sufficient information.

The average frequency-domain stress spectrum, Figure 7, was used in this analysis. The RMS of this spectrum is 2.45 MPa. Sixty-nine (69) percent of the individual spectra had an RMS within 50 percent of this average value. However, large excursions from the mean occurred in many of the individual spectra. The RMS ranged as high as 6.51 MPa in the individual spectra. Sixteen (16) percent had an RMS 100 percent greater than the average, and 4 percent had an RMS 150 percent greater than the average RMS. Rather than trying to duplicate this distribution of the RMS values, we have taken a relatively simplistic and empirical approach to the synthesis of time series. On the basis of our previous experience with synthesis of time series data, we have chosen to vary the RMS of the average spectrum uniformly about its mean value for 95 percent of synthesized time series. For this 95 percent, the spectral amplitude was varied by  $\pm 50$  percent. The remaining 5 percent of the synthesized time series were used to add "large-excursion" cycle counts to "average" cycle counts. The large-excursions were synthesized using a 110 percent increase in the RMS of the average spectrum. As discussed below, this simplified distribution of RMS values produces excellent agreement with the rainflow counted time series data.

The cycle count distribution for the synthesized time series containing the large-excursion data is shown in Figure 9. A similar plot for the mean stress cycle count distribution is shown in Figure 10. As shown in these two figures, the distribution of cycle counts is predicted very well using the frequency-domain technique. Moreover, the distribution in the high-stress tail is also predicted. As discussed in Sutherland,<sup>3</sup> the ability of the frequency synthesis algorithm to generate relatively long time series permits the high-stress tail to be defined. In Reference 3, over 240,000 seconds (66 hours) of synthesized time series data were required to achieve a stable and

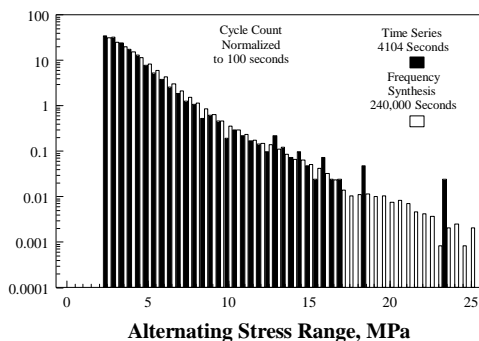


**Figure 9. Alternating Stress Cycle Count Distribution for Measured Data and Synthesized Time Series Data with "Large-Excursions," Root Flap Bending Stress.**

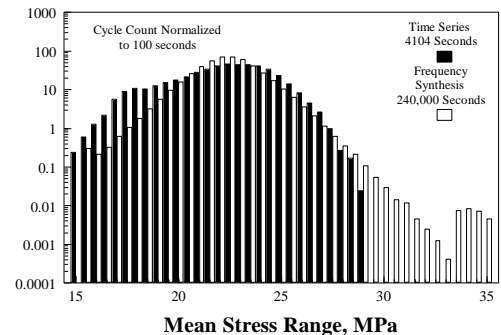


**Figure 10. Mean Stress Cycle Count Distribution for Measured Data and Synthesized Time Series Data with "Large-Excursions," Root Flap Bending Stress.**

relatively smooth distribution of cycle counts in the high-stress tail.

When the counts in the high-stress tail of the synthesized time series data are compared to the counts obtained directly from the 4400 seconds of time series data, the spectral technique predicts more cycles in the high-stress tail of the distribution. The relatively smooth distribution of cycle counts in this high-stress tail is indicative of the relatively long time series, over 240,000 seconds, synthesized for this analysis. As discussed in Sutherland,<sup>3</sup> Thresher, et.al.<sup>6</sup> and Malcolm,<sup>7</sup> the cycle counts from time series data should converge to a relatively smooth distribution as time lengths are increased. The relatively disjoint distribution shown in Figure 9 is a direct result of the relatively short duration (4004 seconds compared with 240,000 seconds) of the time series data. Thus, the distribution and magnitudes of the cycle counts obtained over the alternating stress range using the frequency-domain technique are in excellent agreement with the cycle counts obtained directly from the time series data.

As anticipated, the distribution of mean-stress cycle counts, see Figure 10, is a relatively symmetric distribution, unlike that obtained directly from the time series data. The frequency synthesized data do contain cycles with higher mean stresses. As discussed above, the distribution for the time series data will smooth as the duration of the time series increases. The smoothing of the time series distribution may fill out its distribution. Moreover, a close examination of these high mean-stress cycles shows that they are associated with small alternating-stress cycle ranges. Since determination of service lifetimes is a weak function of mean stress and a strong function of alternating stress, these cycles do not contribute significantly to the accumulation of damage in the blades.

Thus, the distribution and magnitude of cycle counts for the flapwise bending stresses that were obtained from the spectral analysis technique is in excellent agreement with the distribution obtained from the time series data.

### **Root Edgewise Bending Stress**

The cycle count distribution for root edgewise bending stress is significantly different from the distribution for root flap bending stress. As shown in Figures 4 and 6, the root edgewise bending contains a strong, one-per-revolution deterministic (azimuth average) signal (due to the gravity component of the blade loads). These data will be used to illustrate the synthesis of time series data from frequency data containing a strong deterministic signal. For the LIFE2 analysis, the frequency spectrum for the non-deterministic ("random") load is transformed to time series data and then the deterministic signal is added directly to that time series. The total time series is then cycle counted using the rainflow algorithm.

For this analysis, the azimuth average of the in-plane bending stress is determined from the time series data.<sup>5</sup> Then the computed azimuth average of the in-plane signal is subtracted from the time series data as a function of the position of the rotor for each data point in the time series. The resulting time series was then analyzed, as described above, to yield an average amplitude spectrum. The resulting frequency-domain spectrum is equivalent to that shown in Figure 7 without the peaks.

Using the assumed  $\pm 50$  percent variation in the spectral amplitude and the inclusion of the 5 percent large-exursion data, the synthesized time series data for approximately 240,000 seconds (66 hours) yield the cycle count distribution shown in Figures 11 and 12. Again, a comparatively long synthesis procedure was required to achieve a relatively smooth and stable distribution of cycle counts in the high-stress tail. As shown in Figure 11 and discussed above, the distribution and magnitudes of the cycle counts obtained using the frequency-domain techniques are in excellent agreement with the cycle count distribution obtained directly from the time series data. The distribution and magnitude of in-plane mean stress cycle counts, Figure 12, are in good agreement with the distribution and magnitude obtained directly from the in-plane time series data. The frequency-domain technique does produce more high mean-stress cycles. However, as discussed above, these high mean-stress cycles are associated with small alternating-stress ranges. Thus, these cycles do not contribute significantly to the accumulation of damage in the blades.

## DISCUSSION

On the basis of the comparisons presented in Figures 9 through 12, the synthesis of time series data from an average frequency spectrum is an effective technique for the determination of stress cycles imposed on a wind turbine component. The HAWT data analyzed here, and the vertical axis wind turbine (VAWT) data analyzed by Sutherland,<sup>3</sup> illustrate that the frequency-domain analysis is an effective technique for both classes of turbines. However, as discussed by Sutherland,<sup>3</sup> the frequency-domain technique permits this distribution to be defined only within the accuracy of the input frequency spectrum.

## SUMMARY

A set of algorithms permitting the analysis of frequency-domain stress spectra has been incorporated into the LIFE2 fatigue/fracture analysis code for turbine components. The results presented here provide the wind turbine designer with two techniques for determining the cycle-counts from average frequency-

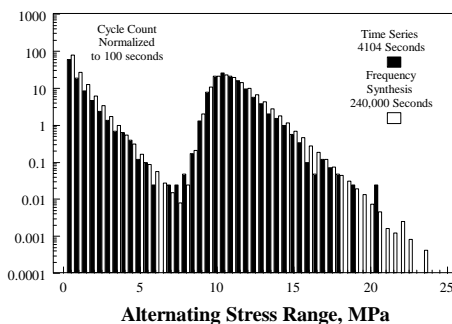


**Figure 11. Alternating Stress Cycle Count Distribution for Measured Data and Synthesized Time Series Data with "Large Excursions," Root Edge Bending Stress.**

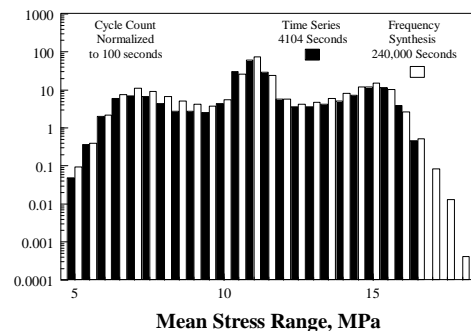


**Figure 12. Mean Stress Cycle Count Distribution for Measured Data and Synthesized Time Series Data with "Large Excursions," Root Edge Bending Stress.**

domain stress spectra. These results further illustrate the accuracy that a designer can expect from the various cycle-counting techniques as well as the importance of relatively long time series data in determining the high-stress tail of the distribution of the stress cycles.

## ACKNOWLEDGMENTS

The authors wish to thank K. Urban for processing and reducing the NPS master analog data tapes into the scaled engineering data cited in this report.

## BIBLIOGRAPHY

1. H. J. Sutherland and L. L. Schluter, "The LIFE2 Computer Code, Numerical Formulation and Input Parameters," Proceedings of WindPower '89, SERI/TP-257-3628, September 1989, pp. 37-42.
2. H. J. Sutherland and L. L. Schluter, "Fatigue Analysis of WECS Components Using a Rainflow Counting Algorithm," Proceedings of Windpower '90, AWEA, Washington, DC, September 1990, pp. 85-92.
3. H. J. Sutherland, "Frequency-Domain Stress Prediction Algorithm for the LIFE2 Fatigue Analysis Code," Proceedings of the Eleventh ASME Wind Energy Symposium, P. S Veers and S. Hock (eds), SED-Vol. 11, ASME, January 1992, pp. 107-113.
4. C. Coleman and B. McNiff, Final Report: Dynamic Response Testing of the Northwind 100 Wind Turbine, Subcontractor Report, SERI Cooperative Research Agreement #DE-FC02-86CH10311, Solar Energy Research Institute, Golden, CO, December 1989, 40 pp.
5. T. Olsen, WINDATDS, Wind Data Analysis Tool Set: User's Manual, Solar Energy Research Institute, Golden, CO, September 1990, 148 pp.
6. R. W. Thresher, S. M. Hock and R. M. Osgood, "Data Record Length Effects on Rainflow Analysis," Proceedings of the Eleventh ASME Wind Energy Symposium, P. S Veers and S. Hock (eds), SED-Vol. 11, ASME, January 1992, p. 117.
7. D. J. Malcolm, "Predictions of Peak Fatigue Stresses in a Darrieus Rotor Wind Turbine Under Turbulent Winds," Proceedings of the Ninth ASME Wind Energy Symposium, D. E. Berg (ed), SED-Vol. 9, ASME, January 1990, pp. 125-135.